

# Electrochemical Properties of Li-Zn Alloy Electrodes Prepared by Kinetically Controlled Vapor Deposition for Lithium Batteries

Zhong Shi,<sup>a,\*</sup> Meilin Liu,<sup>a,\*z</sup> and James L. Goleb

<sup>a</sup>School of Materials Science and Engineering, Georgia Institute of Technology, Atlanta, Georgia 30332-0245, USA

<sup>b</sup>School of Physics, Georgia Institute of Technology, Atlanta, Georgia 30332-0432, USA

A Li-Zn alloy electrode prepared by a kinetically controlled vapor deposition (KCVD) is examined for use as the negative electrode for rechargeable lithium batteries. Results indicate that filamentary or dendritic growth of lithium on a Li-Zn alloy electrode prepared by the KCVD technique are dramatically suppressed due to fast diffusion of lithium in the alloy electrode, suggesting that the Li-Zn prepared by the KCVD method may be used effectively to improve the rechargeability of negative electrodes.  
© 2000 The Electrochemical Society. S1099-0062(00)02-103-9. All rights reserved.

Manuscript submitted February 25, 2000; revised manuscript received April 10, 2000. Available electronically May 22, 2000.

Lithium alloy electrodes have been studied over the last two decades for use as negative electrodes for room-temperature secondary lithium batteries.<sup>1,2</sup> A renewed interest has arisen in lithium alloy electrodes as alternatives to carbon-based intercalation materials following the development of tin-based composite oxides as negative electrodes for Li batteries.<sup>3</sup> Compared with carbonaceous compounds, lithium alloys have a high energy density (both volumetric and gravimetric) and high power density due to their high lithium diffusivity.<sup>4-6</sup> The major drawbacks associated with Li alloys as negative electrodes include Li dendrite formation during charging and large volume change during alloying-de-alloying of Li into/from metallic matrices. This usually results in a fast disintegration (cracking and crumbling) of the alloy electrode.<sup>4</sup> Studies have also shown that the microstructure and morphology of Li alloys, *e.g.*, the grain size, shape, and orientation of the active materials or the reinforcement by nonactive materials in multiphase alloys strongly affect the cycling behavior of lithium alloy electrodes.<sup>7-9</sup>

The most popular method for preparing a binary Li alloy electrode is to electroplate a metallic host matrix onto a substrate (*e.g.*, Cu or Ni) from an aqueous solution at room temperature; Li is then deposited on the metal by electrodeposition in a Li<sup>+</sup>-containing organic electrolyte. This process makes it easy to control the composition, thickness, and morphology of the host matrix, but only a thin layer of the Li alloy can be formed. Another method for preparing a Li alloy is to heat two metals of interest to a predetermined temperature. Using this method, it is relatively easy to form the desired composition of the product alloy. However, it is difficult to control the microstructure and morphology of the alloy because it is usually necessary to melt both metals. Recently, we have developed a system to produce Li alloy films using a variation of the physical vapor deposition process called kinetically controlled vapor deposition (KCVD) method.<sup>10,11</sup> The kinetically controlled lithiation process was developed for the preparation of Li-Mg alloys with controlled microstructure including grain size, orientation, composition, and porosity. By independently controlling the temperature of a molten Li source and a source of solid metal soluble in Li (*e.g.*, Mg, Zn, etc.), films of specific composition can be fabricated. Further, the temperature of the substrate can be varied to control the morphology of the grain structure of the vapor-deposited film. Using this approach, it is possible to couple the bulk diffusivity of Li in the alloy with significantly enhanced surface diffusion due to the formation of Li-based alloys with highly porous structures. As a result, the diffusion of Li in the alloy should be sufficiently fast so that the activity of Li at the electrode interface will remain less than unity to prevent dendrite formation. Recently, we have prepared Li-Zn alloys using the KCVD method. We report

here our initial results on the electrochemical behavior of these Li-Zn alloys.

## Experimental

Zinc rod (diam 0.5 in.), zinc foil, and lithium rod (> 98%) were purchased from Alfa Inorganics. Lithium ribbons (0.38 mm thick, 99.9%) from Aldrich were used as reference and counter electrodes for the electrochemical measurements. The configuration used for the KCVD process, as depicted in Fig. 1, represents an improved modification of our previous design.<sup>10</sup> Here, the Zn disk heated by a thermal coax heating element was mounted in an intermediate chamber above the Li crucible. Li vapor, heated in a lower crucible (again with second thermal coax), would interact with the Zn metal and was mixed with the resulting vaporizing Zn. This Li and Zn mixture then condensed onto the temperature-controlled substrate. The Zn and Li sources were maintained at two different temperatures using the two independent control loops of an Omega CN3000 temperature controller. The maximum temperatures of the solid Zn disk and Li metal in the KCVD configuration were 376 and 500°C, respectively. The Ta sheet, which acted as the deposition substrate, was cooled using

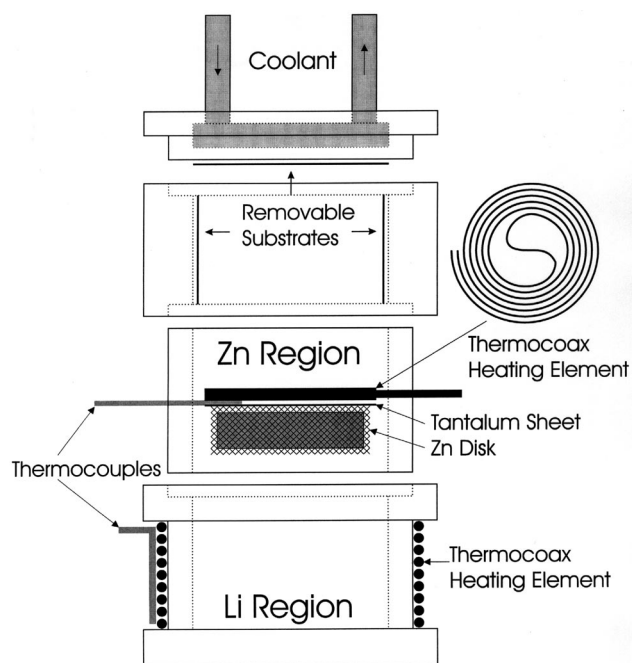


**Figure 1.** A schematic configuration used for forming Li-Zn alloys using KCVD

\* Electrochemical Society Active Member.

<sup>z</sup> E-mail: Meilin.Liu@mse.gatech.edu

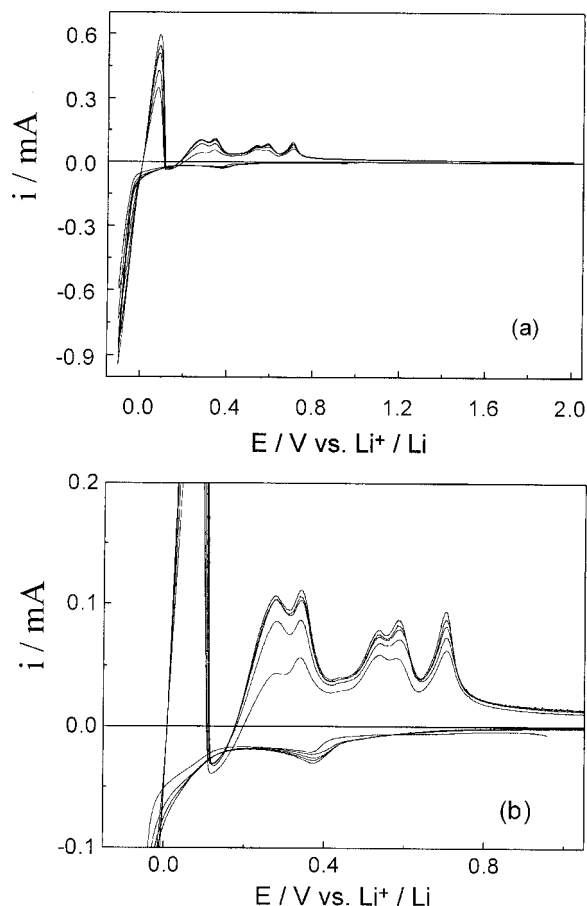


**Figure 2.** CVs of a pure Zn electrode in 1 M LiN(CF<sub>3</sub>SO<sub>2</sub>)<sub>2</sub> EC/DMC (1:2 by volume) with a scan rate of 1 mV/s. (a) The first five cycles in a wide potential range and (b) the redox peaks in the potential range of -0.1 to 1.0 V.

dry ice-methanol slush (the temperature of the substrate was ~-20°C). The Li vapor pressure at the temperature of these experiments ranges from ~10<sup>-3</sup> to 10<sup>-2</sup> Torr.

The microstructure and surface morphology of the Li-Zn alloys were characterized using a scanning electron microscope (SEM, Hitachi S-800). The alloys were then transferred under vacuum to a glove box (Vacuum Atmospheres Company), where a three-electrode electrochemical cell was employed for the electrochemical measurements presented in this paper. The reference and counter electrode were made of lithium foils and a 1 M LiN(SO<sub>2</sub>CF<sub>3</sub>)<sub>2</sub> ethylene carbonate/dimethyl carbonate (EC/DMC) (1:2 by volume) solution was used as the electrolyte. The apparent surface area of the alloy electrodes was 0.2 cm<sup>2</sup>. Two layers of Celgard 2400 film were used as separators. The EC and DMC were dried for at least 24 h with activated 4A molecular sieves. Cyclic voltammetry and galvanostatic intermittent titration technique (GITT) were performed using a Solatron 1285 system controlled by a personal computer.

### Results and Discussion

**Electrochemical behavior of a pure Zn electrode.**—It was necessary to evaluate the electrochemical behavior of pure Zn metal before we studied the electrochemical properties of Li-Zn alloy electrodes. Figure 2 shows the cyclic voltammograms (CVs) of a pure Zn electrode in 1 M LiN(SO<sub>2</sub>CF<sub>3</sub>)<sub>2</sub> EC/DMC (1:2 by volume) at a scan rate of 1 mV/s between 2.0 and -0.1 V. When the potential was scanned in the cathodic direction from 2.0 to -0.1 V, we found one small peak near 0.4 V, as clearly seen in Fig. 2b, corresponding to

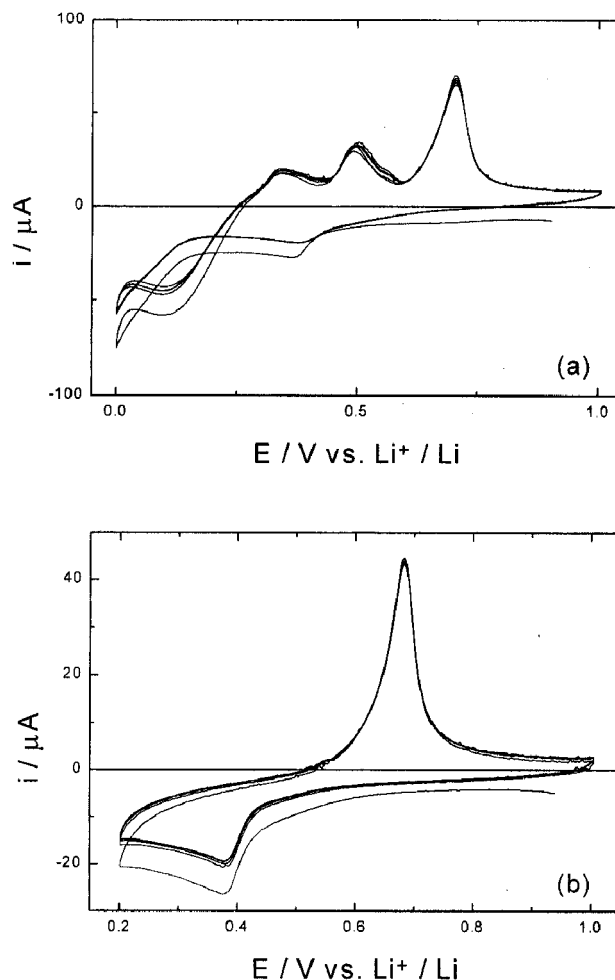


**Figure 3.** CVs of a pure Zn electrode in 1 M LiN(CF<sub>3</sub>SO<sub>2</sub>)<sub>2</sub> EC/DMC (1:2 by volume) with a scan rate of 1 mV/s in the potential range of (a) 1.0 to 0 V and (b) 1.0 to 0.2 V.

cathodic formation of a Li-Zn alloy. The cathodic current then increased dramatically when the potential fell below 0 V, corresponding to the deposition of pure Li onto the electrode surface. Note that the shape of the cathodic current response below 0 V suggests that the active electrode area was increasing dramatically during Li deposition, an indication of Li dendrite formation.

In the anodic direction, we observed a large peak at about 0.08 V, which corresponds to the anodic dissolution of plated pure Li from the electrode, and several peaks in the potential range of 0.2 to 0.8 V, which correspond to the formation of different Li<sub>x</sub>Zn (*x* = 1.5, 1, 0.67, 0.5, 0.4) phases as more Li is removed from the electrode.<sup>5,12</sup> The peak currents increased during the first three cycles and then remained relatively constant thereafter.

When the potential was swept between 1.0 and 0 V, three anodic peaks were observed at 0.35, 0.5, and 0.7 V, respectively, as shown in Fig. 3a. While the cathodic current peak near 0.4 V (corresponding to the alloying process of Li and Zn metal) is still present, the large peak corresponding to deposition of pure Li has disappeared. The complicated shape in the potential range from 0.25 to 0 V may be related to the formation of an additional Li-Zn alloy. It is interesting to note that when the potential was scanned between 1.0 and 0.2 V, only one pair of redox peaks was observed, as shown in Fig. 3b. The anodic peak at 0.68 V corresponds to the formation of Li<sub>2</sub>Zn<sub>5</sub><sup>13</sup> whereas the cathodic peak near 0.4 V corresponds to the formation of LiZn<sub>2</sub>.<sup>13</sup>

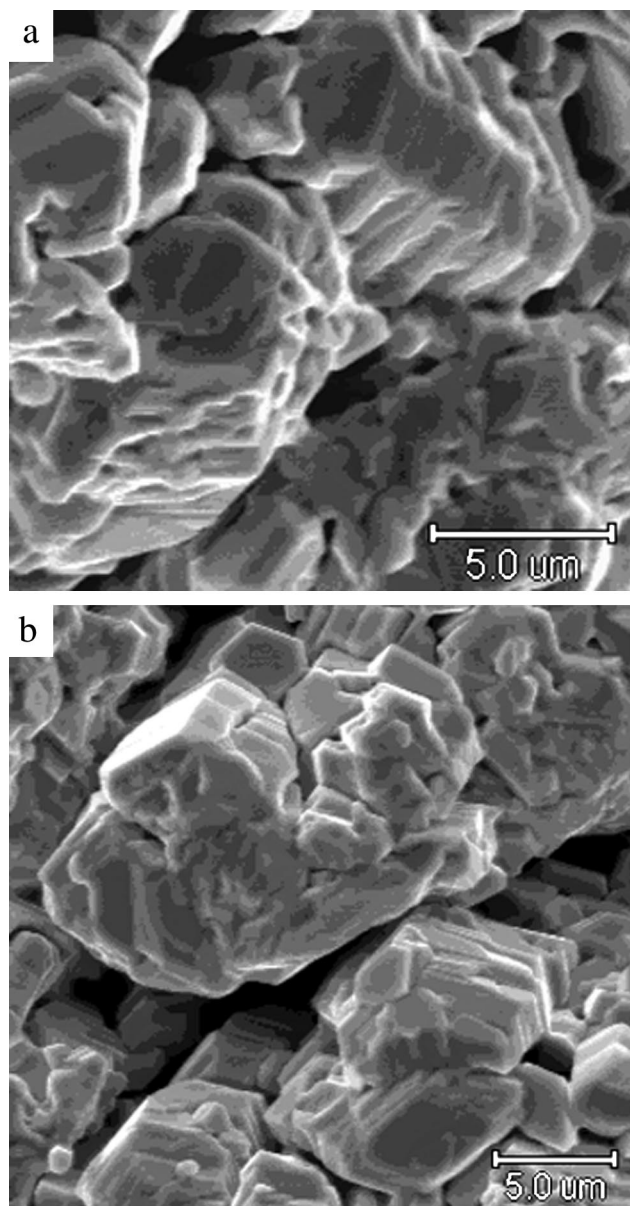


**Figure 4.** SEMs of a Li-Zn alloy prepared by the KCVD method: (a) top view and (b) cross-sectional view.

*Microstructure and surface morphology of a Li-Zn alloy prepared by KCVD.*—Figure 4 shows some typical SEM micrographs of a Li-Zn alloy electrode deposited on a Ta substrate. In contrast to the Li-Mg alloys prepared by a KCVD method,<sup>10,11</sup> the Li-Zn sample does not display a columnar or tapered structure. Instead, it consists of aggregate particles and displays a porous structure. This is beneficial to the passage of liquid electrolyte into the pores to assist mass transfer; further, the real contact area between the liquid electrolyte and the Li-Zn alloy electrode surface will be increased when the alloy film is used as an anode in a Li battery.

As demonstrated in a previous study of Li-Mg alloys,<sup>10</sup> the composition, microstructure, and morphology of the Li-Zn alloy films produced by the KCVD method can be readily controlled through independent variation of the temperature of each source metal together with the temperature of the substrate. These microscopic features greatly influence the electrochemical properties of the alloy electrodes, as discussed elsewhere for Li-Mg alloy electrodes.<sup>11</sup>

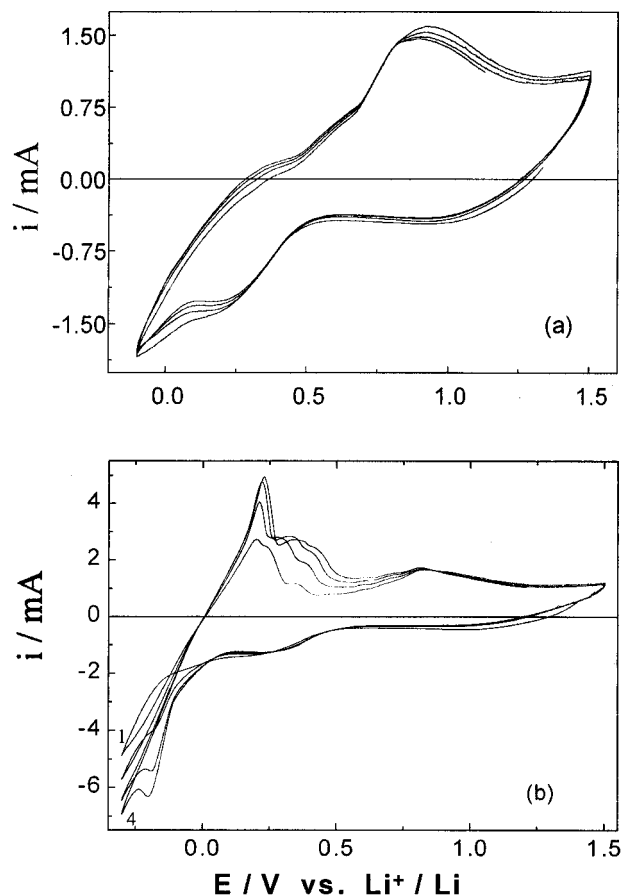


**Figure 5.** C-Vs of a Li-Zn alloy electrode prepared by the KCVD method (the thickness was 0.41 mm) in 1 M LiN(CF<sub>3</sub>SO<sub>2</sub>)<sub>2</sub> EC/DMC (1:2 by volume) with a scan rate of 1 mV/s in the potential range of (a) 1.5 to -0.1 V and (b) 1.5 to -0.3 V.

*Electrochemical properties of a Li-Zn alloy prepared by KCVD.*—Figure 5 shows the CVs of a Li-Zn alloy electrode prepared by the KCVD method. These CV curves differ significantly from those observed on a pure Zn electrode or an electrodeposited Li-Zn alloy electrode<sup>13</sup> (Fig. 2 and 3). First, only one pair of redox peaks is observed in the potential range from 1.5 and -0.1 V, as shown in Fig. 5a, suggesting that the electrochemical behavior of the electrode is dominated by one phase in the Li-Zn system or there is only one Li-Zn phase under these conditions. Second, when the potential was scanned to -0.1 V, no peaks corresponding to the deposition/stripping of pure Li (e.g., current rings in Fig. 2) were observed, implying that the filamentary and dendritic growths that are usually associated with pure Li have essentially been suppressed. These voltammograms are indicative of good cycling behavior of the alloy electrode.

When the potential limit in the anodic direction was lowered to -0.3 V, there was a small current ring in the first cycle, as shown in Fig. 5b; however, the current ring disappeared in subsequent cycles as a new cathodic peak appeared at about -0.18 V, corresponding to cathodic formation of another Li-Zn phase. This cathodic peak at about -0.18 V and the anodic peak at about 0.24 V represent another pair of redox peaks, corresponding to the alloying and dealloying of Li into and from the LiZn phase in the Li-Zn system.<sup>13</sup> The anodic peak corresponding to the Li<sub>2</sub>Zn<sub>3</sub> phase (at about 0.3 V) was also observable under these conditions.

The chemical diffusion coefficients of lithium into the Li-Zn alloy were also measured using the GITT.<sup>14,15</sup> For the Li-Zn alloy

prepared by the KCVD method, the diffusion coefficient of Li is about  $4.7 \times 10^{-8}$  cm<sup>2</sup>/s, which is one order of magnitude larger than those for the LiZn phase prepared by direct alloying, *i.e.*, by melting appropriate amounts of the constituents together to form an alloy.<sup>15</sup>

### Conclusions

The observed electrochemical behavior of a Li-Zn alloy prepared by the KCVD method indicates that the tendency for Li dendrite formation is significantly reduced on such a Li-Zn alloy electrode. The measured diffusivity of Li in the Li-Zn alloy prepared by the KCVD method is much greater than those of Li-Zn alloys prepared by other techniques. These observations suggest that Li-Zn alloys prepared by the KCVD method may be used to effectively prevent dendrite formation, improving the cyclability of Li electrodes and the rechargeability of Li batteries as a result of their high diffusion coefficient. However, the optimization of a Li-Zn alloy electrode with a high diffusivity and good microstructure is still under investigation and will be reported in subsequent communications.

### Acknowledgment

The authors gratefully acknowledge the financial support of this work by CALEB Corporation and the donors of The Petroleum Research Funds, administered by the American Chemical Society (ACS-PRF no. 32792-AC5).

*The Georgia Institute of Technology assisted in meeting the publication costs of this article.*

### References

1. B. M. L. Rao, R. W. Francis, and H. W. Christopher, *J. Electrochem. Soc.*, **124**, 1490 (1977).
2. J. O. Besenhard, *J. Electroanal. Chem.*, **94**, 81 (1978).
3. Y. Idota, T. Kubota, A. Maekawa, and T. Miyasaka, *Science*, **176**, 1395 (1997).
4. J. O. Besenhard, J. Yang, and M. Winer, *J. Power Sources*, **68**, 87 (1997).
5. J. Wang, P. King, and R. A. Huggins, *Solid State Ionics*, **20**, 185 (1986).
6. J. Wang, I. D. Raistrick, and R. A. Huggins, *J. Electrochem. Soc.*, **133**, 457 (1986).
7. J. O. Besenhard, H. P. Fritz, E. Wudy, K. Dietz, and H. Meyer, *J. Power Sources*, **14**, 193 (1985).
8. J. O. Besenhard, P. Komenda, A. Paxinos, E. Wudy, and M. Josowicz, *Solid State Ionics*, **18/19**, 823 (1986).
9. J. Yang, M. Winter, and J. O. Besenhard, *Solid State Ionics*, **90**, 281 (1996).
10. F. Dudel, J. L. Gole, T. A. Sanders, J. King, and R. F. Browner, *Philos. Mag. B*, **75**, 733 (1997).
11. Z. Shi, M. Liu, D. Naik, and J. L. Gole, *J. Power Sources*, Accepted.
12. *Binary Alloy Phase Diagrams*, Vol. 2, T. B. Massalski, Editor, p.1151 (1986).
13. T. Fujieda, S. Takahashi, and S. Heguchi, *J. Power Sources*, **40**, 283 (1992).
14. W. Weppner and R. A. Huggins, *J. Electrochem. Soc.*, **124**, 1569 (1977).
15. A. Anani, S. Crouch-Baker, and R. A. Huggins, in *Lithium Batteries*, A. N. Dey, Editor, PV 87-1, p. 365, The Electrochemical Society Proceedings Series, Pennington, NJ (1987).